# Spin Swapping Effect of Band Structure Origin in Centrosymmetric Ferromagnets

Hyeon-Jong Park,[1] Hye-Won Ko,[2] Gyungchoon Go,[2] Jung Hyun Oh,[3] Kyoung-Whan Kim,[4,*] and Kyung-Jin Lee[2,†]
[1]KU-KIST Graduate School of Converging Science and Technology, Korea University, Seoul 02841, Korea
[2]Department of Physics, Korea Advanced Institute of Science and Technology, Daejeon 34141, Korea
[3]Department of Materials Science and Engineering, Korea University, Seoul 02841, Korea
[4]Center of Spintronics, Korea Institute of Science and Technology, Seoul 02792, Korea

(Received 14 October 2021; revised 19 April 2022; accepted 6 June 2022; published 11 July 2022)

We theoretically demonstrate the spin swapping effect of band structure origin in centrosymmetric ferromagnets. It is mediated by an orbital degree of freedom but does not require inversion asymmetry or impurity spin-orbit scattering. Analytic and tight-binding models reveal that it originates mainly from **k** points where bands with different spins and different orbitals are nearly degenerate, and thus it has no counterpart in normal metals. First-principle calculations for centrosymmetric 3*d* transition-metal ferromagnets show that the spin swapping conductivity of band structure origin can be comparable in magnitude to the intrinsic spin Hall conductivity of Pt. Our theory generalizes transverse spin currents generated by ferromagnets and emphasizes the important role of the orbital degree of freedom in describing spin-orbit-coupled transport in centrosymmetric materials.

DOI: 10.1103/PhysRevLett.129.037202

*Introduction.*—The spin Hall effect [1–3] refers to an electric field induced generation of a spin current due to spin-orbit coupling. Underlying mechanisms of the spin Hall effect are classified into intrinsic and extrinsic ones [4]: The intrinsic mechanism corresponds to band structure effects without resorting to impurity scatterings [5–9], whereas the extrinsic one results from spin-orbit-coupled scatterings from impurities [1,10–13]. The intrinsic mechanism has attracted considerable interest from various physics communities. The intrinsic spin Hall effect was originally established for electrons in condensed matter but has also led to extensive studies on the analogous spin Hall effect of light [14] or in a Fermi gas [15] and a cold-atom system [16], suggesting that intrinsic spin-orbit-coupled transport is of broad fundamental interest. As the intrinsic spin Hall effect does, any spin-orbit-coupled transport of band structure origin would attract attention from various communities within and outside of condensed matter physics.

The spin Hall effect is always accompanied by another spin-orbit-coupled transport, known as the spin swapping effect [17]. In contrast to the spin Hall effect that converts a charge current to a spin current, the spin swapping effect converts a spin current (called primary) to another spin current (called secondary). The symmetry of spin swapping currents is distinct from that of spin Hall currents. Depending on the relative directions of spin polarization and the flow of a primary spin current, there are two types of spin swapping current [17]:

$$j_{ji}^{\mathrm{SS}} = \theta_{\mathrm{SS}}^{(1)} j_{ij} \quad \text{for } i \neq j \quad (\text{type I}), \tag{1a}$$

$$j_{kk}^{\mathrm{SS}} = \theta_{\mathrm{SS}}^{(2)} j_{ii} \quad \text{for } i \neq k \quad (\text{type II}), \tag{1b}$$

where $j_{ij}$ ($j_{ij}^{\mathrm{SS}}$) is a primary (secondary) spin current flowing along the $j$ direction with spin $i$, and $\theta_{\mathrm{SS}}^{(1),(2)}$ are the spin swapping angles, which satisfy $\theta_{\mathrm{SS}}^{(1)} = -\theta_{\mathrm{SS}}^{(2)}$ up to first order in spin-orbit coupling. The spin swapping effect has received great attention due to its scientific [18–24] and technological [25–28] significance.

Ferromagnets provide ideal material platforms to explore the spin swapping effect because an electric field naturally generates a primary spin current polarized along the magnetization. Previous theories have focused mainly on extrinsic spin swapping by impurities [17,19–21,23]. Intrinsic one of band-structure origin has also been investigated but only for noncentrosymmetric systems [18,19,22,24], which is irrelevant to centrosymmetric 3*d* transition-metal ferromagnets such as Co, Fe, and Ni. Investigating the spin swapping effect of band structure origin in centrosymmetric ferromagnets is of crucial importance because they are basic materials for experiments. Examining intrinsic spin transport in centrosymmetric systems requires an explicit consideration of the orbital degree of freedom that is currently a subject of extensive research [7–9,29–34].

In this Letter, by treating the orbital and spin degrees of freedom on equal footing, we derive the spin swapping conductivity in centrosymmetric ferromagnets, whose features are qualitatively different from that in nonmagnets. First-principles calculations for Co, Fe, and Ni show that the spin swapping conductivity of band structure origin can be comparable to the intrinsic spin Hall conductivity of Pt,

 

which exhibits the largest spin Hall conductivity among $5d$ heavy metals.

*Spin swapping effect due to orbital textures.*—To provide unique features of our theory in a simple model, we consider a minimal $p$-orbital system with orbital textures [9]. If an orbital-texture-related physics is found to exist in a $p$-orbital system, it should also exist in $d$-orbital systems. We assume the continuous rotational symmetry, which is a good approximation for many cases. The Hamiltonian is $\mathcal{H} = \mathcal{H}_0 + \mathcal{H}_{\rm SO}$:

$$\mathcal{H}_0 = \frac{\hbar^2 k^2}{2m_e} + \frac{\eta k^2}{2m_e} L_k^2 + J\boldsymbol{\sigma}\cdot\mathbf{m}, \tag{2a}$$

$$\mathcal{H}_{\rm SO} = \frac{\alpha}{\hbar}\mathbf{L}\cdot\boldsymbol{\sigma}, \tag{2b}$$

where $\mathcal{H}_0$ consists of the kinetic term, the orbital texture term, and the $s$-$d$ exchange. Here, $k = |\mathbf{k}|$, $\mathbf{k}$ is the crystal momentum, $J$ is the exchange splitting, $\mathbf{m}$ is the unit vector along the magnetization based on the mean-field approximation for local magnetic moments, $\mathbf{L}$ is the orbital angular momentum operator, $\boldsymbol{\sigma}$ is the spin Pauli-matrix vector for itinerant electron spins, $L_k = \hat{\mathbf{k}}\cdot\mathbf{L}$, $m_e$ is the effective electron mass, $\alpha$ is the spin-orbit coupling energy, and the $\eta$-linear term [35] describes the orbital splitting between a radial $p$ orbital ($\langle L_k^2\rangle = 0$) and tangential $p$ orbitals ($\langle L_k^2\rangle \neq 0$). The orbital splitting parameter $\eta$ originates from the difference between $\sigma$ and $\pi$ hopping integrals and thus is nonzero in general. The orbital splitting term corresponds to the crystal splitting energy, which is on the order of eV and thus one of the largest energy scales in solids. The $s$-$d$ model ignores the quantum correlation of localized spins but is widely used to investigate transport of delocalized spins through a magnetized background [21,23,36–40]. This simple model [Eq. (2)] may have a limited quantitative prediction power but gives key insight into a large spin swapping effect of centrosymmetric ferromagnets as evidenced by tight-binding and first-principle calculations in the next sections.

We first diagonalize $\mathcal{H}_0$ and then treat $\mathcal{H}_{\rm SO}$ perturbatively. $\mathcal{H}_0$ is diagonalized by the unitary transform $U_0^\dagger = e^{i\theta_{\mathbf{k}}L_y/\hbar}e^{i\phi_{\mathbf{k}}L_z/\hbar}e^{i\theta_{\mathbf{m}}\sigma_y/2}e^{i\phi_{\mathbf{m}}\sigma_z/2}$ where the angles satisfy $\hat{\mathbf{v}} = (\sin\theta_{\mathbf{v}}\cos\phi_{\mathbf{v}}, \sin\theta_{\mathbf{v}}\sin\phi_{\mathbf{v}}, \cos\theta_{\mathbf{v}})$ for $\hat{\mathbf{v}} = \hat{\mathbf{k}}$ or $\hat{\mathbf{m}}$. The diagonal components of $U_0^\dagger\mathcal{H}_0U_0$ give the energy eigenvalues

$$E^{(0)}_{\mathbf{k}rs} = \frac{\hbar^2k^2}{2m_e} + sJ, \qquad E^{(0)}_{\mathbf{k}ts} = (1+\eta)\frac{\hbar^2k^2}{2m_e} + sJ, \tag{3}$$

where the subscript $r$ ($t$) refers to the radial (tangential) orbital band and $s = \pm 1$ refer to the spin bands. The corresponding eigenstates are $|\psi_{\mathbf{k}rs}\rangle^{(0)} = U^\dagger|m_l = 0, s\rangle$ and $|\psi_{\mathbf{k}ts}\rangle^{(0)} = U^\dagger|m_l = \pm 1, s\rangle$ for $s = \pm 1$, where $|m_l, s\rangle$ is the eigenstate of $L_z\sigma_z$ with $\langle m_l, s|L_z\sigma_z|m_l, s\rangle = \hbar m_l s$. Despite degenerate tangential bands, the nondegenerate perturbation theory can be applied since $\mathcal{H}_{\rm SO}$ has no matrix element mixing them. Due to its complexity, we do not present perturbed eigenstates $|\psi_{\mathbf{k}ns}\rangle$ and perturbed eigenvalues $E_{\mathbf{k}ns}$ explicitly.

In the presence of an electric field applied along the $x$ direction, the spin-$i$ conductivity flowing to the $j$ direction is given by the Kubo formula: $\sigma^i{}_{jx} = \sum_{\mathbf{k}ns}(\sigma^i{}_{jx})_{\mathbf{k}ns}$ where

$$(\sigma^i_{jx})_{\mathbf{k}ns} = \frac{\hbar e^2}{V}\mathrm{Im}\sum_{n's'}\frac{f_{\mathbf{k}ns} - f_{\mathbf{k}n's'}}{E_{\mathbf{k}ns} - E_{\mathbf{k}n's'}}\frac{[v^i_j]^{\mathbf{k}ns}_{\mathbf{k}n's'}[v_x]^{\mathbf{k}n's'}_{\mathbf{k}ns}}{E_{\mathbf{k}ns} - E_{\mathbf{k}n's'} + i\hbar/\tau}, \tag{4}$$

$f$ is the Fermi-Dirac distribution, $V$ is the system volume, $e$ is the electron charge, $v_i = (1/\hbar)\partial\mathcal{H}/\partial k_i$ is the velocity operator, $v^i_j = \{\sigma_i, v_j\}/2$ is the spin velocity operator, $\hbar/\tau$ is the level broadening, and $[\cdots]^{\mathbf{k}n's'}_{\mathbf{k}ns} = \langle\psi_{\mathbf{k}n's'}|\cdots|\psi_{\mathbf{k}ns}\rangle$.

The type I and II spin swapping conductivities are given by $\sigma^{(1)}_{{\rm SS},\mathbf{k}ns} = (\sigma^x_{zx})_{\mathbf{k}ns}$ for $\mathbf{m} = \hat{\mathbf{z}}$ and $\sigma^{(2)}_{{\rm SS},\mathbf{k}ns} = (\sigma^z_{zx})_{\mathbf{k}ns}$ for $\mathbf{m} = \hat{\mathbf{x}}$, respectively [23], which have different geometries from the spin Hall conductivity $\sigma_{\rm SH} = \sigma^y_{zx}$. We calculate the conductivities for radial orbital bands $[(n, s) = (r, \pm)]$ since tangential bands exhibit similar features. Up to first order in $\alpha$, we obtain

$$\sigma^{(1)}_{{\rm SS},\mathbf{k}r\pm} = -\sigma^{(2)}_{{\rm SS},\mathbf{k}r\pm} = \frac{\alpha}{J}\frac{\eta\Delta_{\mathbf{k}}}{2\Delta_{\mathbf{k}} \mp \eta}\sigma_{{\rm SP},\mathbf{k}r\pm}, \tag{5}$$

where $\sigma_{{\rm SP},\mathbf{k}rs}[= (\sigma^i_{xx})_{\mathbf{k}ns} = (\partial_E f_{\mathbf{k}ns})\hbar^2k^2e^2\tau/3m_e^2V]$ corresponds to the primary spin-polarized conductivity for $\hat{\mathbf{i}} = \hat{\mathbf{m}}$ and $\Delta_{\mathbf{k}} = 2m_eJ/\hbar^2k^2$. Equation (5) gives the spin swapping conductivity of band structure origin, which originates from a concerted action between the orbital texture ($\eta$) and the exchange interaction ($\Delta_{\mathbf{k}}$), both of which are intrinsic in ferromagnets. We note that our model does not include spin-orbit scattering by impurities [$\propto\boldsymbol{\sigma}\cdot(\mathbf{k}\times\nabla\mathcal{V})$ where $\mathcal{V}$ is the impurity potential], which drives extrinsic spin swapping effects [19–21,23]. Equation (5) is an intraband contribution [41] originating from the anomalous velocity from the orbital texture term in Eq. (2a), which is completely different from the orbital Hall effect [42].

When $2\Delta_{\mathbf{k}} \approx \pm\eta$ is satisfied, Eq. (5) yields particularly large contributions to the spin swapping conductivity. This condition is equivalent to $E^{(0)}_{\mathbf{k}t\pm} \approx E^{(0)}_{\mathbf{k}r\mp}$, i.e., two bands with different spins and different orbitals are nearly degenerate. We call the $\mathbf{k}$ values satisfying this condition *hot spots*, which would be present as points or lines in the $\mathbf{k}$ space. The standard nondegenerate perturbation theory breaks down at these hot spots, but the spin swapping conductivity does not diverge as shown by a degenerate perturbation theory [43]. The spin swapping angles [Eq. (1)] at the hot spots are mostly determined by a single-band property since $|2\Delta_{\mathbf{k}} \mp \eta|^{-1} \gg |2\Delta_{\mathbf{k}} \pm \eta|^{-1}$ for $2\Delta_{\mathbf{k}} \approx \pm\eta$ so that

$\theta_{SS}^{(1)} = -\theta_{SS}^{(2)} \approx \alpha\eta\Delta_{\mathbf{k}}/J(2\Delta_{\mathbf{k}} \mp \eta)$. It is notable that the orbital-mediated spin swapping current may travel long distance without suffering from strong spin dephasing because the Fermi wave vectors for the spin majority and the spin minority bands are very close to the hot spots, in stark contrast to the conventional transverse spin current [47].

The hot-spot feature is widely valid for the following reasons. Since the spin-orbit coupling Hamiltonian includes terms $\propto L_+S_- + L_-S_+$, any pair of bands satisfying the selectionlike rule $\Delta m_l + \Delta s = 0$ with a small energy difference introduces hot spots. Since the orbital splitting and the exchange interaction are both on the order of eV, hot spots would appear in wide ranges of ferromagnets. Note that the selectionlike rule makes sense only when the orbital and spin degrees of freedom are taken into account on equal footing, instead of integrating out one of them first [9,48]. This is a clear difference from spin-orbit-coupled transport in centrosymmetric nonmagnets for which the orbital and spin degrees of freedom can be considered separately [8,9] (see the Supplemental Material [43] for model details).

*Tight-binding model calculation.*—The spin swapping effect of band structure origin in centrosymmetric ferromagnets is not limited to the toy model including the *ad hoc* orbital splitting term $\eta L_k^2$. To demonstrate this, we adopt a minimal $sp^3$ tight-binding model in a cubic lattice: $\mathcal{H} = \mathcal{H}_L + J\boldsymbol{\sigma}\cdot\mathbf{m} + (\alpha/\hbar)\mathbf{L}\cdot\boldsymbol{\sigma}$, which is an $8\times 8$ matrix ($sp^3$ orbitals for spin up or down). The exchange and spin-orbit interactions in $\mathcal{H}$ are described by on site terms. $\mathcal{H}_L$, which corresponds to the kinetic term, includes the hopping terms of $s$ and $p$ orbitals, with different magnitudes of $\sigma$ and $\pi$ hoppings and $sp$ hybridization, whose explicit matrix elements are shown in the Supplemental Material [43].

In Fig. 1(a), we plot the band structure along the high symmetry points for $\mathbf{m} = \hat{\mathbf{z}}$. The following parameters are used (all values are in the unit of eV): the on site energy of $s$ orbital $E_s = -2.0$, that of $p$ orbital $E_p = 1.0$, the hopping integral of $s$ orbital $t_s = -0.25$, the $\sigma$ and $\pi$ hopping integrals of $p$ orbital, $t_{p\sigma} = 0.4$ and $t_{p\pi} = -0.2$, respectively, the $sp$ hybridization $\gamma_{sp} = 0.4$, the exchange splitting $J = 0.1$, and the spin-orbit coupling $\alpha = 0.03$. The top four (bottom two) bands are the tangential (radial) $p$ bands. There are anticrossing points between majority-tangential bands and minority-radial bands as indicated by green arrows.

We calculate the spin conductivity [Eq. (4)] using the Green's function formalism [35,49], whose details are presented in the Supplemental Material [43]. The energy dependence of type I spin swapping conductivity ($\sigma_{SS}^{(1)} = \sigma_{zx}^{x}$) [Fig. 1(b)] shows that it has the maximum at $E = 0.992$ eV, where the majority-tangential and minority-radial bands are nearly degenerate. To demonstrate the hot-spot feature, we compute $\mathbf{k}$-resolved $\sigma_{SS}^{(1)}$ and

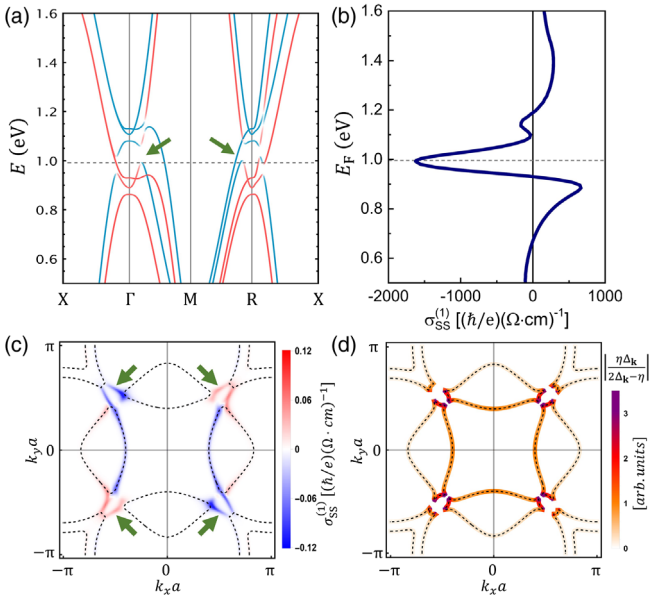


FIG. 1. Tight-binding calculation. (a) Band structure. Blue (red) curves correspond to spin-minority (spin-majority) bands. (b) Energy dependence of type I spin swapping conductivity $\sigma_{SS}^{(1)}$. In (a) and (b), dashed horizontal lines at $E = 0.992$ eV correspond to the maximum $\sigma_{SS}^{(1)}$. $\mathbf{k}$-resolved (c) $\sigma_{SS}^{(1)}$ summed over all the bands and (d) $|\eta\Delta_{\mathbf{k}}/(2\Delta_{\mathbf{k}} - \eta)|$ at $k_z a = 1.655$, $E = 0.992$ eV, and $a = 2$ Å. Green arrows in (a) and (c) correspond to anticrossing points. $|\eta\Delta_{\mathbf{k}}/(2\Delta_{\mathbf{k}} - \eta)|$ of (d) is computed in equilibrium and without spin-orbit coupling.

$|\eta\Delta_{\mathbf{k}}/(2\Delta_{\mathbf{k}} - \eta)|$. Dominant contributions to $\sigma_{SS}^{(1)}$ originate from colored $\mathbf{k}$ points [Fig. 1(c)], at which $|\eta\Delta_{\mathbf{k}}/(2\Delta_{\mathbf{k}} - \eta)|$ is also large [Fig. 1(d)]. These $\mathbf{k}$ points correspond to the hot spots where the energy gap between the majority-tangential band and minority-radial band is small. The close correlation between $\mathbf{k}$-resolved $\sigma_{SS}^{(1)}$ [Fig. 1(c)] and $|\eta\Delta_{\mathbf{k}}/(2\Delta_{\mathbf{k}} - \eta)|$ supports the hot-spot feature predicted by the toy model.

*First-principles calculations for Co, Fe, and Ni.*—We perform the density functional theory calculations for centrosymmetric $3d$ transition-metal ferromagnets (Fe, Co, and Ni). We use the OpenMX package [50], which is based on a norm-conserving pseudopotential [51] and pseudoatomic localized basis function [50]. We choose the generalized gradient approximation [52] for the exchange-correlation functional and use the pseudo-atomic basis orbitals $s2p2d2$. The crystal structures are body-centered cubic for Fe, and face-centered cubic for Co and Ni where the lattice constants are experimental values (2.86 Å for Fe, 3.54 Å for Co, and 3.52 Å for Ni). The $\mathbf{k}$-point meshes are $22\times 22\times 22$ for Fe, and $18\times 18\times 18$ for Co and Ni. From the computed ground state solutions, we obtain spin conductivities from the same formalism used in the tight-binding calculation where the Hamiltonian is replaced by the ground state Hamiltonian with the atomic orbital

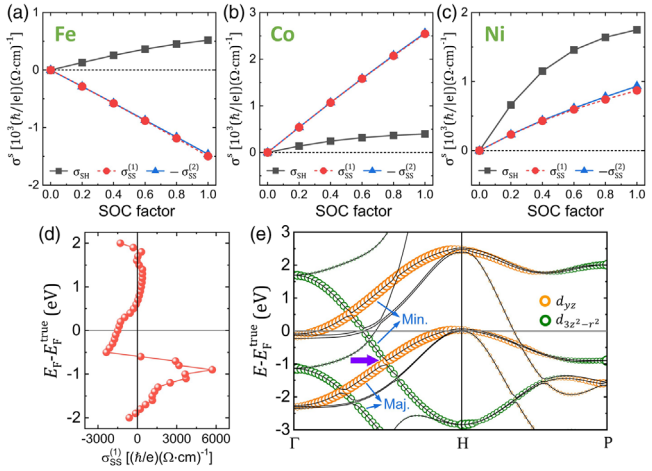


FIG. 2. The spin Hall conductivity $\sigma_{\mathrm{SH}}$ (black dashed) and the two types of spin swapping conductivities $\sigma_{\mathrm{SS}}^{(1),(2)}$ (red and blue respectively) as a function of a normalized spin-orbit coupling parameter (SOC factor) for (a) Fe, (b) Co, and (c) Ni. (d) Computed $\sigma_{\mathrm{SS}}^{(1)}$ in the energy range of $-2.0$ eV to 2.0 eV for Fe. (e) The band structure along the Γ–H–P path in the first Brillouin zone for Fe. The size of the circles indicates the magnitude of $d_{yz}$ (orange) and $d_{3z^2-r^2}$ (green) orbital characters. The purple arrow indicates the anticrossing between the spin-minority $d_{3z^2-r^2}$ and spin-majority $d_{yz}$ orbital bands. Maj. means spin majority band whereas Min. means spin minority band.

basis. We use $251 \times 251 \times 251$ $\mathbf{k}$-point mesh for computing spin conductivities where the $\mathbf{k}$-point convergence is obtained. We use the level broadening $\delta$ of 25 meV because this $\delta$ value gives longitudinal conductivities comparable to experimental values at room temperature.

In Figs. 2(a)–2(c), we present calculated spin Hall conductivity $\sigma_{\mathrm{SH}}$ and spin swapping conductivities $\sigma_{\mathrm{SS}}^{(1),(2)}$ as a function of spin-orbit coupling strength (divided by the true spin-orbit coupling strength). The magnetization is along the $z$ axis for calculating $\sigma_{\mathrm{SH}} = \sigma_{zx}^{y}$ (black dashed) and $\sigma_{\mathrm{SS}}^{(1)} = \sigma_{zx}^{x}$ (red), and is along the $x$ axis for calculating $\sigma_{\mathrm{SS}}^{(2)} = \sigma_{zx}^{z}$ (blue). Calculated $\sigma_{\mathrm{SH}}$'s of ferromagnets are similar to those in the literature [53]. We find that $\sigma_{\mathrm{SS}}^{(1),(2)}$ are similar in magnitude to $\sigma_{\mathrm{SH}}$. In contrast, the extrinsic spin swapping effect is about 1 order of magnitude smaller than the spin Hall effect [23]. Therefore, the mechanism of band structure origin can generate much stronger spin swapping currents than the extrinsic spin-orbit scatterings from impurities. Moreover, $\sigma_{\mathrm{SS}}^{(1),(2)}$ of Co is $\sim 2500$ $(\hbar/e)$ $(\Omega\,\mathrm{cm})^{-1}$. This value is larger than $\sigma_{\mathrm{SH}}$ of Pt [$\sim 2000$ $(\hbar/e)$ $(\Omega\,\mathrm{cm})^{-1}$] [54]. Another point of Figs. 2(a)–2(c) is that $\sigma_{\mathrm{SS}}^{(1)}$ is very similar to but slightly different from $-\sigma_{\mathrm{SS}}^{(2)}$. We attribute this small difference to higher-order spin-orbit coupling effects because $\sigma_{\mathrm{SS}}^{(1)} \equiv -\sigma_{\mathrm{SS}}^{(2)}$ is guaranteed up to first order of spin-orbit coupling [17].

We next calculate $\sigma_{\mathrm{SS}}^{(1)}$ for Fe as a function of the Fermi energy [Fig. 2(d)] to demonstrate that spin swapping of band structure origin in realistic materials is mediated by the hot spots. $\sigma_{\mathrm{SS}}^{(1)}$ has a peak around $E - E_F \approx -1.0$ eV. This peak structure of $\sigma_{\mathrm{SS}}^{(1)}$ versus $E - E_F$ is qualitatively the same even when the spin-orbit coupling parameter becomes 3 times larger than the true value [43]. Figure 2(e) shows the orbital-resolved band structure along the Γ–H–P path. Here, the size of circles indicates the magnitude of the $d_{yz}$ character (orange) and $d_{3z^2-r^2}$ character (green). It clearly shows that the spin-minority $d_{3z^2-r^2}$ and spin-majority $d_{yz}$ orbital bands make an anticrossing around $E - E_F \approx -1.0$ eV (purple arrow). Note that this anticrossing satisfies $\Delta m_l + \Delta s = 0$ and results in a hot spot. On the other hand, the anticrossing near $E - E_F \approx 0.5$ eV does not satisfy $\Delta m_l + \Delta s = 0$ (since both bands are spin minority) so that it does not yield a peak of $\sigma_{\mathrm{SS}}^{(1)}$. The peak of spin swapping conductivity at the hot spot justifies the validity of our theory for realistic materials. Moreover, the peak structure of the spin swapping conductivity indicates that it can be enhanced by tuning the Fermi level. The first-principles calculations for Co and Ni exhibit similar features [43].

*Discussions.*—In this Letter, we theoretically demonstrate the spin swapping effect of band structure origin in centrosymmetric ferromagnets. We find that the spin swapping conductivity is sizable for $3d$ transition-metal ferromagnets such as Co, Fe, and Ni, which are widely examined in experiments. The large spin swapping effect in centrosymmetric ferromagnets is found to originate from hot spots where two bands with different spins and different orbitals are nearly degenerate. As the hot-spot feature arises in any ferromagnets, we expect that the large spin swapping effect may also exist in ferromagnets other than centrosymmetric $3d$ transition-metal ferromagnets.

We note that the hot-spot feature is not limited to the spin swapping effect, but is far more general for transverse spin transport. For instance, we confirm that the intrinsic spin Hall conductivity calculated in the same model [Eq. (2)] shares the same hot spots [43]. A previous study [53] also shows a peak structure of the intrinsic spin Hall conductivity of ferromagnets near anticrossing points between majority and minority bands. This is a crucial difference from spin transport in nonmagnets. In nonmagnets, the absence of exchange splitting makes the spin bands degenerate at any $\mathbf{k}$ points, so that the selectionlike rule (for two bands with *different* spins and different orbitals) cannot be applied. Rather, the intrinsic spin Hall phenomena in nonmagnets are closely related to the orbital transport through spin-orbit coupling [9]. In ferromagnets, however, the orbital transport and the spin transport mainly originate from different spots in $\mathbf{k}$ space. The former originates from the mixture of two bands with the *same* spins and different orbitals (due to orbital hybridization),

while the latter does mainly from the mixture of two bands with *different* spins and different orbitals (due to spin-orbit coupling).

Finally, we discuss the practical importance of large spin swapping conductivity for spin-orbit torque applications [55–59]. Recent experiments on ferromagnetic trilayers, consisting of in-plane ferromagnet/normal metal/perpendicular ferromagnet, have demonstrated field-free spin-orbit torque switching of perpendicular magnetization [26–28]. Note that these experiments employed centrosymmetric ferromagnets. The field-free switching is realized by a spin current polarized along the $z$ direction and flowing in the $z$ direction, i.e., $j_{zz}$. The original interpretation for $j_{zz}$ is the interfacial spin-orbit precession [26], of which existence was confirmed by first-principle calculations [60]. We note that the type II spin swapping effect also contributes to $j_{zz}$. For an in plane ferromagnet magnetized along the $x$ direction, a primary spin current $j_{xx}$ naturally arises, which in turn generates a secondary $j_{zz}$ through the spin swapping process in the ferromagnet bulk. As the field-free spin-orbit torque switching of perpendicular magnetization is of technological relevance [61–69] and $j_{zz}$ can substantially reduce the field-free switching current [70], our result suggests that the large spin swapping effect of centrosymmetric ferromagnets must be further exploited to realize spin-orbit torque applications.

We thank A. Manchon for fruitful discussion. K.-J. L. was supported by the Samsung Research Funding Center of Samsung Electronics under Project No. SRFCMA1702-02. K.-W. K. was supported by the National Research Foundation of Korea (NRF) funded by the Ministry of Science and ICT (2020R1C1C1012664) and the KIST Institutional Programs (2E31541, 2E31542).

*kwk@kist.re.kr
†kjlee@kaist.ac.kr

[1] M. I. Dyakonov and V. I. Perel, Possibility of orienting electron spins with current, JETP Lett. **13**, 467 (1971), http://jetpletters.ru/ps/1587/article_24366.shtml.
[2] Y. K. Kato, R. C. Myers, A. C. Gossard, and D. D. Awschalom, Observation of the spin Hall effect in semiconductors, Science **306**, 1910 (2004).
[3] J. Wunderlich, B. Kaestner, J. Sinova, and T. Jungwirth, Experimental Observation of the Spin-Hall Effect in a Two-Dimensional Spin-Orbit Coupled Semiconductor System, Phys. Rev. Lett. **94**, 047204 (2005).
[4] J. Sinova, S. O. Valenzuela, J. Wunderlich, C. H. Back, and T. Jungwirth, Spin Hall effects, Rev. Mod. Phys. **87**, 1213 (2015).
[5] S. Murakami, N. Nagaosa, and S.-C. Zhang, Dissipationless quantum spin current at room temperature, Science **301**, 1348 (2003).
[6] J. Sinova, D. Culcer, Q. Niu, N. A. Sinitsyn, T. Jungwirth, and A. H. MacDonald, Universal Intrinsic Spin Hall Effect, Phys. Rev. Lett. **92**, 126603 (2004).
[7] T. Tanaka, H. Kontani, M. Naito, T. Naito, D. S. Hirashima, K. Yamada, and J. Inoue, Intrinsic spin hall effect and orbital hall effect in $4d$ and $5d$ transition metals, Phys. Rev. B **77**, 165117 (2008).
[8] H. Kontani, T. Tanaka, D. S. Hirashima, K. Yamada, and J. Inoue, Giant Intrinsic Spin and Orbital Hall Effects in $Sr_2MO_4$ ($M$ = Ru, Rh, Mo), Phys. Rev. Lett. **100**, 096601 (2008).
[9] D. Go, D. Jo, C. Kim, and H.-W. Lee, Intrinsic Spin and Orbital Hall Effects from Orbital Texture, Phys. Rev. Lett. **121**, 086602 (2018).
[10] J. E. Hirsch, Spin Hall Effect, Phys. Rev. Lett. **83**, 1834 (1999).
[11] S. Zhang, Spin Hall Effect in the Presence of Spin Diffusion, Phys. Rev. Lett. **85**, 393 (2000).
[12] M. Gradhand, D. V. Fedorov, P. Zahn, and I. Mertig, Extrinsic Spin Hall Effect from First Principles, Phys. Rev. Lett. **104**, 186403 (2010).
[13] A. Ferreira, T. G. Rappoport, M. A. Cazalilla, and A. H. Castro Neto, Extrinsic Spin Hall Effect Induced by Resonant Skew Scattering in Graphene, Phys. Rev. Lett. **112**, 066601 (2014).
[14] X. Ling, X. Zhou, K. Huang, Y. Liu, C.-W. Qiu, H. Luo, and S. Wen, Recent advances in the spin Hall effect of light, Rep. Prog. Phys. **80**, 066401 (2017) and references therein.
[15] L. W. Cheuk, A. T. Sommer, Z. Hadzibabic, T. Yefsah, W. S. Bakr, and M. W. Zwierlein, Spin-Injection Spectroscopy of a Spin-Orbit Coupled Fermi Gas, Phys. Rev. Lett. **109**, 095302 (2012).
[16] M. C. Beeler, R. A. Williams, K. Jiménez-Garca, L. J. LeBlanc, A. R. Perry, and I. B. Spielman, The spin Hall effect in a quantum gas, Nature (London) **498**, 201 (2013).
[17] M. B. Lifshits and M. I. Dyakonov, Swapping Spin Currents: Interchanging Spin and Flow Directions, Phys. Rev. Lett. **103**, 186601 (2009).
[18] S. Sadjina, A. Brataas, and A. G. Mal'shukov, Intrinsic spin swapping, Phys. Rev. B **85**, 115306 (2012).
[19] K. Shen, R. Raimondi, and G. Vignale, Theory of coupled spin-charge transport due to spin-orbit interaction in inhomogeneous two-dimensional electron liquids, Phys. Rev. B **90**, 245302 (2014).
[20] H. B. M. Saidaoui, Y. Otani, and A. Manchon, Crossover between spin swapping and Hall effect in disordered systems, Phys. Rev. B **92**, 024417 (2015).
[21] H. B. M. Saidaoui and A. Manchon, Spin-Swapping Transport and Torques in Ultrathin Magnetic Bilayers, Phys. Rev. Lett. **117**, 036601 (2016).
[22] J. Borge and I. V. Tokatly, Ballistic spin transport in the presence of interfaces with strong spin-orbit coupling, Phys. Rev. B **96**, 115445 (2017).
[23] C. O. Pauyac, M. Chshiev, A. Manchon, and S. A. Nikolaev, Spin Hall and Spin Swapping Torques in Diffusive Ferromagnets, Phys. Rev. Lett. **120**, 176802 (2018).
[24] S. Li, K. Shen, and K. Xia, Interfacial spin Hall effect and spin swapping in Fe-Au bilayers from first principles, Phys. Rev. B **99**, 134427 (2019).
[25] A. M. Humphries, T. Wang, E. R. J. Edwards, S. R. Allen, J. M. Shaw, H. T. Nembach, J. Q. Xiao, T. J. Silva, and X. Fan, Observation of spin-orbit effects with spin rotation symmetry, Nat. Commun. **8**, 911 (2017).

[26] S. C. Baek, V. P. Amin, Y.-W. Oh, G. Go, S.-J. Lee, G.-H. Lee, K.-J. Kim, M. D. Stiles, B.-G. Park, and K.-J. Lee, Spin currents and spinorbit torques in ferromagnetic trilayers, Nat. Mater. **17**, 509 (2018).

[27] Y.-W. Oh, J. Ryu, J. Kang, and B.-G. Park, Material and thickness investigation in ferromagnet/Ta/CoFeB trilayers for enhancement of spinorbit torque and field-free switching, Adv. Electron. Mater. **5**, 1900598 (2019).

[28] J. Ryu, R. Thompson, J. Y. Park, S.-J. Kim, G. Choi, J. Kang, H. B. Jeong, M. Kohda, J. M. Yuk, J. Nitta, K.-J. Lee, and B.-G. Park, Efficient spinorbit torque in magnetic trilayers using all three polarizations of a spin current, Nat. Electron. **5**, 217 (2022).

[29] V. T. Phong, Z. Addison, S. Ahn, H. Min, R. Agarwal, and E. J. Mele, Optically Controlled Orbitronics on a Triangular Lattice, Phys. Rev. Lett. **123**, 236403 (2019).

[30] J. Zhu, J.-J. Su, and A. H. MacDonald, Voltage-Controlled Magnetic Reversal in Orbital Chern Insulators, Phys. Rev. Lett. **125**, 227702 (2020).

[31] S. Bhowal and S. Satpathy, Intrinsic orbital moment and prediction of a large orbital Hall effect in two-dimensional transition metal dichalcogenides, Phys. Rev. B **101**, 121112 (R) (2020).

[32] W.-Y. He, D. Goldhaber-Gordon, and K. T. Law, Giant orbital magnetoelectric effect and current-induced magnetization switching in twisted bilayer graphene, Nat. Commun. **11**, 1650 (2020).

[33] T. P. Cysne, M. Costa, L. M. Canonico, M. B. Nardelli, R. B. Muniz, and T. G. Rappoport, Disentangling Orbital and Valley Hall Effects in Bilayers of Transition Metal Dichalcogenides, Phys. Rev. Lett. **126**, 056601 (2021).

[34] S. Bhowal and G. Vignale, Orbital Hall effect as an alternative to valley Hall effect in gapped graphene, Phys. Rev. B **103**, 195309 (2021).

[35] H.-W. Ko, H.-J. Park, G. Go, J. H. Oh, K.-W. Kim, and K.-J. Lee, Role of orbital hybridization in anisotropic magnetoresistance, Phys. Rev. B **101**, 184413 (2020).

[36] L. Berger, Exchange interaction between ferromagnetic domain wall and electric current in very thin metallic films, J. Appl. Phys. **55**, 1954 (1984).

[37] G. E. Volovik, Linear momentum in ferromagnets, J. Phys. C **20**, L83 (1987).

[38] G. Tatara and H. Fukuyama, Resistivity Due to a Domain Wall in Ferromagnetic Metal, Phys. Rev. Lett. **78**, 3773 (1997).

[39] S. Zhang, P. M. Levy, and A. Fert, Mechanisms of Spin-Polarized Current-Driven Magnetization Switching, Phys. Rev. Lett. **88**, 236601 (2002).

[40] K.-W. Kim and K.-J. Lee, Generalized Spin Drift-Diffusion Formalism in the Presence of Spin-Orbit Interaction of Ferromagnets, Phys. Rev. Lett. **125**, 207205 (2020).

[41] The factor $(2\Delta_{\mathbf{k}} \mp \eta)^{-1}$ in Eq. (5) originates from the perturbation with respect to the spin-orbit coupling, not the interband transition due to the electric field.

[42] D. Go, F. Freimuth, J.-P. Hanke, F. Xue, O. Gomonay, K.-J. Lee, S. Blugel, P. M. Haney, H.-W. Lee, and Y. Mokrousov, Theory of current-induced angular momentum transfer dynamics in spin-orbit coupled systems, Phys. Rev. Research **2**, 033401 (2020).

[43] See Supplemental Material at http://link.aps.org/supplemental/10.1103/PhysRevLett.129.037202, which include Refs. [44–46], for detailed discussions on the degenerate perturbation theory, the difference of spin-orbit-coupled transport between nonmagnets and ferromagnets, the tight-binding model, first-principles calculations for Co and Ni, and the analytic calculation of the spin Hall conductivity.

[44] J. C. Slater and G. F. Koster, Simplified LCAO method for the periodic potential problem, Phys. Rev. **94**, 1498 (1954).

[45] R. Lake, G. Klimeck, R. C. Bowen, and D. Jovanovic, Single and multiband modeling of quantum electron transport through layered semiconductor devices, J. Appl. Phys. **81**, 7845 (1997).

[46] S. Datta, *Electronic Transport in Mesoscopic System* (Cambridge University Press, Cambridge, England, 1997).

[47] M. D. Stiles and A. Zangwill, Anatomy of spin-transfer torque, Phys. Rev. B **66**, 014407 (2002).

[48] H. Kontani, T. Tanaka, and K. Yamada, Intrinsic anomalous Hall effect in ferromagnetic metals studied by the multi-*d*-orbital tight-binding model, Phys. Rev. B **75**, 184416 (2007).

[49] S. Ghosh and A. Manchon, Spin-orbit torque in a three-dimensional topological insulatorferromagnet heterostructure: Crossover between bulk and surface transport, Phys. Rev. B **97**, 134402 (2018).

[50] T. Ozaki, Variationally optimized atomic orbitals for large-scale electronic structures, Phys. Rev. B **67**, 155108 (2003).

[51] G. B. Bachelet, D. R. Hamann, and M. Schlüter, Pseudopotentials that work: From H to Pu, Phys. Rev. B **26**, 4199 (1982).

[52] J. P. Perdew, K. Burke, and M. Ernzerhof, Generalized Gradient Approximation Made Simple, Phys. Rev. Lett. **77**, 3865 (1996).

[53] V. P. Amin, J. Li, M. D. Stiles, and P. M. Haney, Intrinsic spin currents in ferromagnets, Phys. Rev. B **99**, 220405(R) (2019).

[54] G. Y. Guo, S. Murakami, T.-W. Chen, and N. Nagaosa, Intrinsic Spin Hall Effect in Platinum: First-Principles Calculations, Phys. Rev. Lett. **100**, 096401 (2008).

[55] I. M. Miron, K. Garello, G. Gaudin, P.-J. Zermatten, M. V. Costache, S. Auffret, S. Bandiera, B. Rodmacq, A. Schuhl, and P. Gambardella, Perpendicular switching of a single ferromagnetic layer induced by in-plane current injection, Nature (London) **476**, 189 (2011).

[56] L. Liu, C.-F. Pai, Y. Li, H. W. Tseng, D. C. Ralph, and R. A. Buhrman, Spin-torque switching with the giant spin Hall effect of tantalum, Science **336**, 555 (2012).

[57] A. Manchon, J. Železný, I. M. Miron, T. Jungwirth, J. Sinova, A. Thiaville, K. Garello, and P. Gambardella, Current-induced spin-orbit torques in ferromagnetic and antiferromagnetic systems, Rev. Mod. Phys. **91**, 035004 (2019).

[58] W. Wang, T. Wang, V. P. Amin, Y. Wang, A. Radhakrishnan, A. Davidson, S. R. Allen, T. J. Silva, H. Ohldag, D. Balzar, B. L. Zink, P. M. Haney, J. Q. Xiao, D. G. Cahill, V. O. Lorenz, and Xin Fan, Anomalous spinorbit torques in magnetic single-layer films, Nat. Nanotechnol. **14**, 819 (2019).

[59] D. Céspedes-Berrocal, H. Damas, S. Petit-Watelot, D. Maccariello, P. Tang, A. Arriola-Córdova, P. Vallobra, Y. Xu, J.-L. Bello, E. Martin, S. Migot, J. Ghanbaja, S. Zhang, M. Hehn, S. Mangin, C. Panagopoulos, V. Cros, A. Fert, and J.-C. Rojas-Sánchez, Current-induced spin torques on single GdFeCo magnetic layers, Adv. Mater. **33**, 2007047 (2021).

[60] V. P. Amin, J. Zemen, and M. D. Stiles, Interface-Generated Spin Currents, Phys. Rev. Lett. **121**, 136805 (2018).

[61] G. Yu, P. Upadhyaya, Y. Fan, J. G. Alzate, W. Jiang, K. L. Wong, S. Takei, S. A. Bender, L.-T. Chang, Y. Jiang, M. Lang, J. Tang, Y. Wang, Y. Tserkovnyak, P. Khalili Amiri, and K. L. Wang, Switching of perpendicular magnetization by spin-orbit torques in the absence of external magnetic fields, Nat. Nanotechnol. **9**, 548 (2014).

[62] A. van den Brink, G. Vermijs, A. Solignac, J. Koo, T. Kohlhepp, H. J. M. Swagten, and B. Koopmans, Field-free magnetization reversal by spin-Hall effect and exchange bias, Nat. Commun. **7**, 10854 (2016).

[63] S. Fukami, C. Zhang, S. DuttaGupta, A. Kurenkov, and H. Ohno, Magnetization switching by spin-orbit torque in an antiferromagnet-ferromagnet bilayer system, Nat. Mater. **15**, 535 (2016).

[64] Y.-W. Oh, S. C. Baek, Y. M. Kim, H. Y. Lee, K.-D. Lee, C.-G. Yang, E.-S. Park, K.-S. Lee, K.-W. Kim, G. Go, J.-R. Jeong, B.-C. Min, H.-W. Lee, K.-J. Lee, and B.-G. Park, Field-free switching of perpendicular magnetization through spin-orbit torque in antiferromagnet/ferromagnet/oxide structures, Nat. Nanotechnol. **11**, 878 (2016).

[65] Y.-C. Lau, D. Betto, K. Rode, J. M. D. Coey, and P. Stamenov, Spin-orbit torque switching without an external field using interlayer exchange coupling, Nat. Nanotechnol. **11**, 758 (2016).

[66] K. Cai, M. Yang, H. Ju, S. Wang, Y. Ji, B. Li, K. W. Edmonds, Y. Sheng, B. Zhang, N. Zhang, S. Liu, H. Zheng, and K. Wang, Electric field control of deterministic current-induced magnetization switching in a hybrid ferromagnetic/ferroelectric structure, Nat. Mater. **16**, 712 (2017).

[67] J. Ryu, S. Lee, K.-J. Lee, and B.-G. Park, Current-induced spin-orbit torques for spintronic applications, Adv. Mater. **32**, 1907148 (2020).

[68] H. C. Koo, S. B. Kim, H. Kim, T.-E. Park, J. W. Choi, K.-W. Kim, G. Go, J. H. Oh, D.-K. Lee, E.-S. Park, I.-S. Hong, and K.-J. Lee, Rashba effect in functional spintronic devices, Adv. Mater. **32**, 2002117 (2020).

[69] L. Liu, C. Zhou, X. Shu, C. Li, T. Zhao, W. Lin, J. Deng, Q. Xie, S. Chen, J. Zhou, R. Guo, H. Wang, J. Yu, S. Shi, P. Yang, S. Pennycook, A. Manchon, and J. Chen, Symmetry-dependent field-free switching of perpendicular magnetization, Nat. Nanotechnol. **16**, 277 (2021).

[70] D.-K. Lee and K.-J. Lee, Spin-orbit torque switching of perpendicular magnetization in ferromagnetic trilayers, Sci. Rep. **10**, 1772 (2020).